

# Inexpensive optical tweezers for undergraduate laboratories

Stephen P. Smith, Sameer R. Bhalotra, Anne L. Brody, Benjamin L. Brown,  
Edward K. Boyda, and Mara Prentiss

*Department of Physics, Harvard University, Cambridge, Massachusetts 02138*

(Received 9 July 1997; accepted 6 July 1998)

Single beam gradient force optical traps, or tweezers, are a powerful tool for a wide variety of experiments in physics, chemistry, and biology. We describe how to build an optical tweezer with a total cost of  $\approx \$6500$  using only commercially available optics and mounts. We also suggest measurements that could be made using the apparatus. © 1999 American Association of Physics Teachers.

## I. INTRODUCTION

Light is a powerful tool for manipulating microscopic objects. It can control the position and orientation of objects as large as  $100\ \mu\text{m}$  and as small as a single atom. Light force, in the form of single beam gradient force traps, has been used to trap and manipulate dielectric spheres,<sup>1</sup> viruses, bacteria,<sup>2</sup> living cells,<sup>2,3</sup> organelles,<sup>4-6</sup> colloidal gold,<sup>7</sup> and even DNA.<sup>8</sup> Such traps, or optical tweezers, have measured elasticity, force, torsion, position, surface structure,<sup>9</sup> and the interaction between particles.<sup>10</sup> There are a wealth of experiments that are easily performed by undergraduates in which optical tweezers can contribute to important measurements in physics, chemistry, and biology.

Unfortunately, most optical tweezer experiments have used equipment which is beyond the budgets of typical undergraduate laboratories. In the following paper, we present a detailed discussion of a three-dimensional optical tweezer constructed using a 20-mW He-Ne laser and a high school grade microscope and objective, rather than the very expensive microscopes with \$2000 to \$5000 objectives which are typical of most optical tweezer experiments. Further, the entire apparatus is made of commercially available optics and mounts. The assembly of the apparatus requires only screwdrivers and wrenches. No machining is required. A detailed parts list including sources, part numbers, and quantities is provided on our web site at <http://atom.harvard.edu/~tweezer>. The time required for an undergraduate to set up such an optical tweezer is typically 25 h.

With our simple tweezer we have trapped and manipulated a variety of transparent objects: polystyrene spheres with diameters from  $0.08$  to  $20\ \mu\text{m}$ , micron-sized biological specimens such as yeast cells and bacteria, and asymmetrically shaped silicon dioxide objects. The measured transverse trapping efficiency of our tweezer is within a factor of 2 of published results using much more expensive tweezers.<sup>11</sup> The ability to trap polystyrene spheres is more than a convenient demonstration of the optical tweezers; such spheres can be used as handles to manipulate biological particles that are too small to trap directly such as DNA<sup>8</sup> and many viruses.

*Overview:* In Sec. II, the theory underlying optical tweezers is developed and some simple formulas are given for predicting the strength of such traps. In Sec. III, a simple optical tweezer setup will be examined and in Sec. IV the selection criteria for the various parts will be explained. Section V covers the alignment procedure for the trap, and Sec. VI details the operation, optimization, and calibration of the trap. Section VII suggests a range of experiments that can be done with such a tweezer, and Sec. VIII suggests enhance-

ments to the basic tweezer. Finally, an optics review and procedures for mixing polystyrene ball solutions are included as appendices.

## II. BASIC TWEEZER THEORY

The basic operation of optical tweezers can be explained by the momentum transfer associated with redirection of light at a dielectric interface. Since light carries momentum that is proportional to its energy and in the direction of propagation, the reflection and refraction of light at the interface changes the momentum of the light. If the momentum of the light changes by  $\Delta p$ , conservation of momentum requires that the dielectric must undergo an equal and opposite momentum change  $-\Delta p$ . The resulting force on the dielectric is just the momentum change per second.

The force on the sphere due to the redirection of an incoming ray,  $r_m$ , can be calculated by subtracting the total momentum of the exiting rays,  $\{r_{m_1}, r_{m_2}, \dots\}$ , from the momentum of  $r_m$ , as shown in Fig. 1. The total force due to a light beam can be calculated by representing the light beam as a collection of rays, and summing the force(s) due to each of the rays. Stable trapping requires that there be some position  $\vec{r}_{\text{trap}}$  where the net force on the sphere is zero and any small displacement results in a restoring force toward  $\vec{r}_{\text{trap}}$ .

A qualitative understanding of the trapping force on a dielectric sphere with refractive index greater than the surrounding medium due to a focused light beam can be obtained by considering the momentum change between two incident rays,  $r_1$  and  $r_2$ , their first reflected and refracted rays,  $r_{m_1}$  and  $r_{m_2}$ , respectively, where the incoming light is propagating in the  $z$  direction as shown in Fig. 2(a) and (b). The incident rays make an angle  $\theta$  to the  $z$  axis, lie in a plane, and in the absence of the sphere intersect at the origin, indicated by the closed circle in the figures. For a sphere with a center at  $(0,0,z_0)$ , symmetry causes the  $x$  and  $y$  components of the forces to cancel. In contrast, the  $z$  component of the forces due to the rays add.

In Fig. 2(a) the center of the sphere is located above the origin and the  $z$  component of the force associated with the reflected rays  $r_{11}$  and  $r_{21}$  is in the direction of propagation, pushing the sphere toward the origin. The net force due to the refracted rays,  $r_{12}$  and  $r_{22}$ , is also in the positive  $z$  direction since the projection of the rays onto the  $z$  axis after being refracted by the sphere is smaller than their projection before the sphere.

In Fig. 2(b) the center of the sphere is below the origin. The force due to the reflected rays is still in the positive  $z$  direction; however, in this case it pushes the sphere away

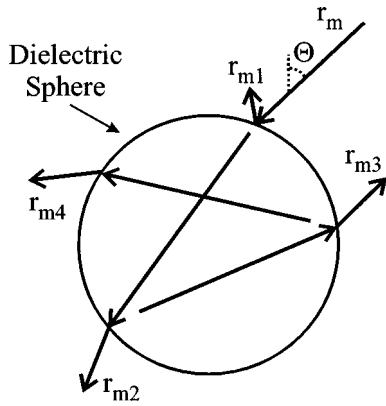


Fig. 1. Ray tracing diagram for a single ray incident on a dielectric sphere of index greater than the surrounding media. The figure shows the incoming ray,  $r_m$ , the reflected ray,  $r_{m1}$ , and the first refracted ray,  $r_{m2}$ , and subsequent refracted rays,  $r_{m3}$  and  $r_{m4}$ .

from the origin. In contrast, the force due to the refracted rays is now in the negative  $z$  direction and pushes the sphere toward the origin. If the force due to the refracted rays is larger than the force due to the reflected rays, then a restoring force and a stable trap will exist. Otherwise, the reflection force will dominate and the sphere will simply be accelerated along the  $z$  axis.

Notice that the net force associated with the refraction of the two rays increases with  $\theta$ , whereas the net force associated with reflection of the two rays decreases with increasing  $\theta$ . Thus the restoring force will be stronger for incoming rays at larger  $\theta$ , and there is a minimum  $\theta$  that is required for stable trapping.<sup>12</sup> A similar analysis will show that a displacement perpendicular to the  $z$  axis also results in a force toward the focus of the rays.

Figure 3 shows the normalized force on a dielectric sphere calculated by considering the forces due to a collection of the incoming rays and all the resulting refracted and reflected rays.<sup>13</sup> The sphere is made of polystyrene ( $n=1.58$ ), suspended in water ( $n=1.33$ ), and illuminated with a tightly focussed Gaussian beam from a microscope objective [numerical aperture (NA)=1.0]. As expected from the previous qualitative argument, the equilibrium position of the sphere in Fig. 3 is slightly below the focus of the beam and the force

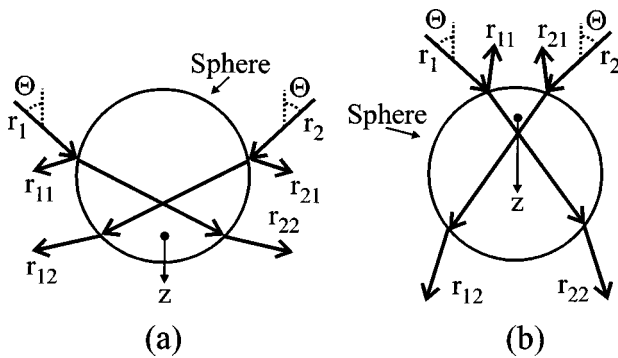


Fig. 2. Simplified ray tracing diagram of the net force on a dielectric sphere displaced above (a), and below (b) the focus of the rays in the absence of the sphere. The figure shows two incoming rays,  $r_1$  and  $r_2$ , the reflected beams,  $r_{11}$  and  $r_{21}$ , and the first refracted beams,  $r_{12}$  and  $r_{22}$ .

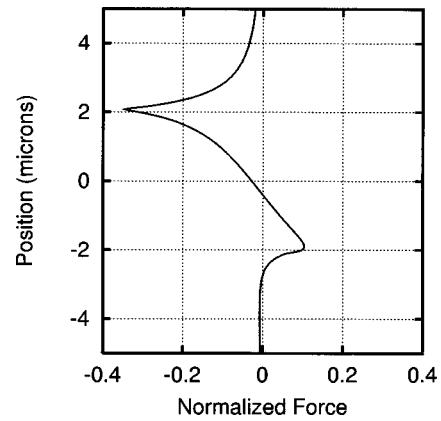


Fig. 3. Normalized force on a sphere as a function of displacement from beam focus. Force is calculated using a ray optics model for a  $3\text{-}\mu\text{m}$  polystyrene sphere suspended in water illuminated by a Gaussian beam with a numeric aperture of 1.0.

required to remove the sphere from the trap is significantly weaker in the  $+z$  direction, the direction of light propagation, than in the  $-z$  direction.

In the discussion above, we used the momentum changes associated with the reflection and refraction of light to provide a qualitative explanation of the trapping force of optical tweezers. It is also possible to derive the trapping force using a different model, based on the Lorentz force exerted by the trapping light on the atoms in the trapped object.<sup>14</sup> The short version of this argument states that the light induces a dipole moment,  $\vec{P}$ , in the material.<sup>15</sup> This induced dipole moment is proportional to the electric field  $\vec{E}$ . The total energy of the induced dipole in the field is then

$$U = -\vec{P} \cdot \vec{E} \propto -\vec{E} \cdot \vec{E} \propto -I,$$

since the intensity,  $I$ , is proportional to the square of the electric field in an isotropic medium with a polarizability that is linear in  $\vec{E}$ . Thus the energy of the particle is a minimum where the intensity is a maximum. For a focused light beam, the intensity maximum occurs at the focus, so particles in such a beam will be attracted to the focus. Since the potential is proportional to  $-I$ , the associated force is proportional to  $\nabla I$ . It is this force that is responsible for the trapping in optical tweezers.

The correspondence between the Lorentz force treatment and the ray tracing treatment can be obtained by recalling that the index of refraction difference that produces reflection and refraction can be derived from a model where the dielectric is composed of an array of bound electrons. The electric field due to the light causes the electrons to oscillate around their equilibrium positions. The acceleration due to this oscillation produces a propagating electric field. The total field propagating in the medium is then the sum of the initial electric field and the electric field radiated by all of the oscillating electrons. The net result is a phase shift of the field in the medium with respect to the field in free space, corresponding to an index of refraction different from 1.<sup>16</sup> Thus our initial method calculated the change in the momentum of the light due to the rescattering of the light by the atoms, and then used momentum conservation to calculate the force on

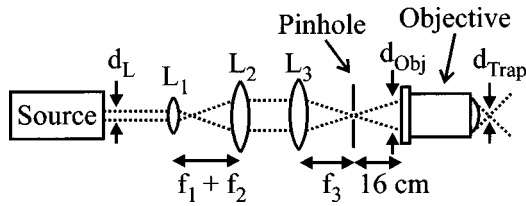


Fig. 4. Schematic diagram of the optical elements of a basic tweezer apparatus.

the atoms. The second treatment, based on the Lorentz force, directly calculates the force on the atoms resulting from the rescattering.

There are several characteristics of an optical trap that can be derived from the discussions above. First, the strength of the trap will increase with the power in the light beam. Second, for a given laser power, the strength of the trap will increase with a decrease in the size of the focused spot,  $w_{\text{trap}}$ , corresponding to an increase in the intensity at the trap. Third, the trap will be weakest in the direction of the beam propagation where the intensity gradient is weakest<sup>17</sup> and the force associated with reflection is opposed to the restoring force.

In the absence of damping, a particle that enters the trap will leave the trap since the force is conservative. In the presence of damping, a particle can lose energy as it enters the trap, so that it does not have enough kinetic energy to escape; however, the fluctuation-dissipation theorem implies that the damping must be accompanied by fluctuations.<sup>18</sup> In order for the particles to stay trapped, the trap depth must be greater than the kinetic energy characteristic of the fluctuations (Brownian motion). For objects suspended in an aqueous medium, viscous drag provides the damping.

To get an idea of the strength of such a trap, consider a simple example. A 10-mW laser is focused to a diffraction limited spot through a 100 $\times$ , numerical aperture 1.25 microscope objective and used to trap 3- $\mu\text{m}$ -diam polystyrene balls suspended in water. The index of refraction of polystyrene is approximately 1.58 and the index of refraction of water is 1.33. The maximum restoring force can be found using the formula from Ref. 19,

$$F = Q \left( \frac{n_1 P}{c_0} \right), \quad (1)$$

where  $F$  is the maximum force exerted by the trap,  $Q$  is a scaling constant that depends on the size of the ball and the index difference between the sphere and the surrounding media and is approximately 0.25 in this case,<sup>19</sup>  $n_1 \approx 1.33$  is the index of refraction of the medium,  $P \approx 10$  mW is the incident power, and  $c_0$  is the speed of light in vacuum. The maximum force from the trap is expected to be approximately 10 pN.

### III. BASIC TWEEZER ELEMENTS

In this section a simplified optical tweezer apparatus will be described. The basic single beam optical tweezer consists of a tightly focused laser beam that traps the object, a sample manipulating system for coarse positioning of the sample, and an imaging system used to monitor the experiment. Schematics of the system are shown in Figs. 4 and 5.

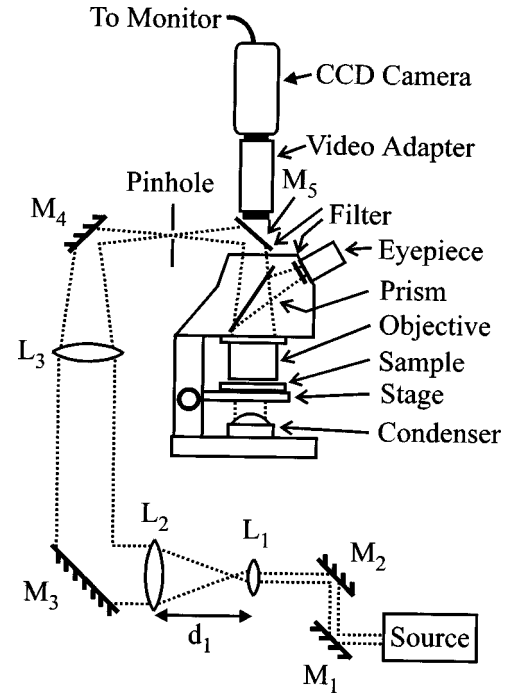


Fig. 5. Simplified schematic diagram of a complete microscope based optical tweezer setup.

#### A. Trapping optics

This section describes a procedure for transforming a given laser beam into a tightly focused spot with the greatest trap depth. Maximizing the trap depth is equivalent to maximizing  $\nabla I$  at the trapping focus. Once the microscope objective and laser are chosen, maximizing the trap depth is equivalent to adjusting the size and curvature of the light incident on the microscope objective so that the objective will focus the light to achieve the maximum possible intensity gradient. A basic schematic of the trapping optics is shown in Fig. 4. Appendix A presents a review of basic ray optics and some fundamental formulas from wave optics.

$\nabla I$  can be increased by decreasing  $w_{\text{trap}}$  as long as the total power is held constant. Unfortunately, the diffraction of the light places a fundamental limit on the value of  $w_{\text{trap}}$  that can be achieved with a particular laser and microscope objective. An ideal lens of focal length  $f$  focusing a collimated laser beam with diameter  $D$  and wavelength  $\lambda_0$  will produce a  $w_{\text{trap}}$  such that

$$\begin{aligned} w_{\text{trap}} &\geq \frac{1.22 f \lambda}{2D} = \frac{1.2 \lambda_0 \tan[\sin^{-1}(\text{NA}/n)]}{n} \\ &= \frac{1.22 \lambda_0}{n} \sqrt{\left( \frac{n}{\text{NA}} \right)^2 - 1}, \end{aligned}$$

where NA is the numerical aperture of the lens, and  $n$  is the index of refraction of the medium. A typical 100 $\times$  microscope oil immersion objective has a numerical aperture of 1.25 resulting in a focused spot of  $w_0 = [1.22(0.63)/(2(1.5))] \sqrt{(1.5/1.25)^2 - 1} = 0.17 \mu\text{m}$  for red light with a wavelength of 0.63  $\mu\text{m}$ .

For a given lens, the trap is strongest when the diameter of the incident light at the objective,  $d_{\text{obj}}$ , is approximately the same as the diameter of the objective,  $D_{\text{obj}}$ .<sup>20</sup> If  $d_{\text{obj}}$

$<D_{\text{obj}}$ ,  $w_{\text{trap}}$  will be greater than the minimum value for the lens, decreasing the strength of the trap. If  $d_{\text{obj}} > D_{\text{obj}}$ , not all the light will be transmitted by the objective. In this case,  $w_{\text{trap}}$  will have the minimal value, but the intensity and the intensity gradient will be lower than for  $d_{\text{obj}} \approx D_{\text{obj}}$ . The diameter of the output of our lasers was smaller than  $D_{\text{obj}}$ , so we used a telescope, formed by lenses  $L_1$  and  $L_2$ , to transform the output of the laser into a collimated beam with a diameter of  $d_{\text{obj}} \approx 0.75$  cm.

Having the correct spot size at the objective is not sufficient for optimal trapping: The laser beam must also have the correct radius of curvature at the objective. Many microscope objectives are designed to achieve the minimum spot size when the radius of curvature of the incoming light is approximately 16 cm. Lens  $L_3$  converts the collimated output of the telescope into a beam with the appropriate size and curvature at the microscope objective. If the focal length of  $L_3$  is 16 cm and the separation between  $L_3$  and the objective is 32 cm, then  $L_3$  will focus the light 16 cm from the back of the objective. The divergence of the light from this focus will result in a light beam at the microscope objective with a radius of curvature of approximately 16 cm and a diameter  $d_{\text{obj}} = D_{\text{obj}}$ . The same divergence can be obtained by diffraction from a pinhole with a  $40\lambda$  diameter, approximately 16 cm from the objective.

## B. Sample manipulating system

We assume that the object to be trapped is suspended in an aqueous solution, which is held between a standard microscope slide and cover slip. Coarse manipulation is done by translating the sample using the microscope stage.

## C. Imaging system

In order to perform experiments, it is necessary to observe the trapped particles. In an apparatus that uses a microscope, the trapping and imaging objectives are the same, as shown in Fig. 5. The light for the imaging is provided by the condenser, which is commonly an integral part of the microscope. It is convenient to image through a dichroic beam-splitter that reflects the trapping light down into the microscope, but transmits some of the imaging light from the condenser up to a charge-coupled device (CCD) camera or a microscope eyepiece.

On microscopes where the video port is used to couple the laser into the objective, as shown in Fig. 5, the regular eyepieces can be used to observe the trapped particles. However, it is *very* important that color filters be used between the objective and the eyepieces to prevent the very intense laser beam from being transmitted to the eyepieces. In Fig. 5, these filters are shown mounted inside the microscope head so that they are difficult to remove inadvertently, but the eyepieces can still be changed as needed. If a visible wavelength laser is used, the trapping beam should be barely visible through the eyepieces even with the trapping laser at maximum power.

For maximum safety, the eyepieces should not be used: All imaging should be done using the video camera. With the laser off, the video camera can be adjusted to match the focus and field of view of the eyepieces, and then the eyepieces can be replaced with firmly secured caps. It is often advantageous to remove the trinocular head of the micro-

scope entirely. This reduces laser losses, stray reflections, and laser hazards. In this case, the video camera must be independently supported.

## IV. CHOOSING COMPONENTS

In this section, detailed selection criteria for the components of the tweezers will be discussed. With other microscopes, lasers, or wavelengths, the selection criteria will remain the same, but the specific values for the required components may be different.

### A. Laser

There are four important characteristics of the laser used for trapping: the output beam shape, the beam astigmatism, the power, and the wavelength. The first two characteristics determine how well a particular microscope objective can focus the laser. In order to focus the optical beam to a single very small spot, the laser should have a single transverse mode output (e.g.,  $\text{TEM}_{00}$ ) with good beam quality.<sup>17</sup> A laser power of between 20 and 100 mW at the microscope is sufficient for many basic trapping experiments.

The preferred laser wavelength depends on the intended uses of the trap. For inanimate objects like polystyrene balls, visible lasers can be used. For biological specimens, the absorption of such a tightly focused visible laser is often large enough to damage the specimen. The absorption of infrared light is significantly less, so sources with wavelengths between 750 and 1000 nm are often used. Fortunately, high power, single transverse mode infrared laser diodes are inexpensive and readily available. Diode pumped solid state lasers with wavelengths around 1000 nm, e.g., Nd:YAG lasers, are more expensive, but also a popular choice.

Most of our experiments were conducted using moderate power (25-mW) red He-Ne lasers, though we have also trapped using green light from an argon laser. Polystyrene spheres could be trapped with powers at the back of the objective as small as 5 mW. The He-Ne and argon lasers had very symmetric output modes and required no spatial filtering.

We have also successfully trapped polystyrene spheres, yeast, and bacteria using infrared diode lasers. Unfortunately, trapping with diode lasers is somewhat more challenging than trapping with visible lasers: The mode from many diode lasers is highly asymmetric; the alignment of infrared sources can be much more difficult than the alignment of visible lasers; and infrared lasers require more laser safety precautions than visible lasers.

The output of a diode laser can be made symmetric and nonastigmatic by spatial filtering using a pinhole or a single mode optical fiber. It was also possible to spatially filter by simply overfilling the rear aperture of the microscope objective with the uncorrected beam from the laser diode. These spatial filtering techniques typically result in power losses of  $\approx 50\%$ . Alternatively, the shape of the beam can be made more symmetrical by selectively expanding (or contracting) the beam along one axis. This can be conveniently done using an anamorphic prism without significant power loss.<sup>21</sup> We have successfully trapped using each of the techniques described above.

### B. Pinhole

For many microscope objectives the diffraction due to a  $\approx 40\lambda$  pinhole 16 cm from the rear of the objective provides

the beam size and radius of curvature that produce the minimal focused spot. For light at  $0.63\ \mu\text{m}$ , a  $25\text{-}\mu\text{m}$  pinhole (for example, Edmund Scientific, Barrington, NJ, No. A36,390) provides good trapping. The best trapping is achieved when the size of the beam at the pinhole is the same as the size of the pinhole. Once the correct beam size is obtained at the pinhole, the pinhole should be removed. If the optical quality of the laser beam is good, the trap depth should remain the same. If the optical quality of the beam is poor, removing the pinhole may decrease the trap depth because it removes the spatial filtering provided by the pinhole. In this case, it is advisable to return the pinhole to the apparatus.

### C. Lenses

As discussed above, the purpose of the telescope is to transform the output of the laser into a collimated beam with a diameter equal to  $D_{\text{obj}}$ , the diameter of the microscope objective. Assuming that the output of the laser is roughly collimated, the magnification,  $M$ , of the telescope should be given by the ratio of  $D_{\text{obj}}$  to the diameter of the output of the laser. For a simple telescope composed of two convex lenses,  $L_1$  and  $L_2$ , with focal lengths  $f_1$  and  $f_2$ , respectively, that are separated by  $d_1 = f_1 + f_2$ , as shown in Fig. 5, and the magnification,  $M$ , is given by  $M = L_2/L_1$ . In order to minimize aberrations, it is advisable to use lenses with focal length  $5\text{ cm} \leq f \leq 40\text{ cm}$  and to use two telescopes if the magnification needs to be larger than 8:1.

All the lenses we used were 1 in. in diameter, standard commercial grade biconvex lenses (Edmund Scientific, Barrington, NJ, Technical grade lenses). Antireflection coatings on the lenses are helpful in reducing transmission losses and stray reflections.

### D. Sending the light through the objective

Finally, the light needs to be sent into the microscope itself. It is convenient to do this through a video port, if the microscope is equipped with one. Otherwise, it can be sent in through one of the eyepiece holders after the eyepiece itself has been removed. It is convenient to use two mirrors in adjustable mounts to center the laser light on the objective and make the light perpendicular to the objective.

### E. Objective

We use a  $100\times$  objective with a 1.25 numerical aperture that requires the use of index matching oil between the microscope objective and the cover slip. We have used both plan and semiplan objectives and have not observed a significant difference between their trapping performance. We used standard “student” grade objectives priced between \$100 and \$500 (e.g., Edmund Scientific, Barrington, NJ, No. A38344). While trapping is possible with lower magnification or lower numerical aperture objectives, it is more difficult and therefore they are not recommended.

### F. Sample manipulation

A standard microscope slide and cover slip makes a convenient container for trapping objects suspended in an aqueous medium. A translator is then required to move the sample. For many applications, the stage provided with the microscope is adequate. For some high precision applications where submicron control is desired, the stage should be

supplemented with or replaced by a finer translator. Also, very fine changes in the position of trapped particles can be achieved by changing the alignment of the laser into the objective.

### G. Imaging system

The trapping objective can also be used by the imaging system. The imaging light can be provided by the microscope condenser, or by another light source such as a fiber-optic lamp. Since the trapping light and the imaging light pass through the same objective, the trapped particle can be viewed either through a CCD camera or one of the microscope eyepieces. In either case, color filters are *absolutely* required to reduce the intensity of the trapping beam to an acceptable level. This is important to prevent damage to the CCD camera and even more important to prevent permanent irreparable eye damage if an eyepiece is used. A dichroic beamsplitter chosen for your laser wavelength can be used as a color filter since it will reflect most of the trapping light but transmit some of the imaging light. This permits the two beams to follow the same path through the objective, but allows only the imaging light to reach the viewers. However, depending on the reflectivity of the dichroic beamsplitter, a second or even a third filter may be required to reduce the trapping light to an acceptable level.

## V. BASIC TRAP ALIGNMENT PROCEDURE

In this section, the procedure for the initial layout and alignment of the trap will be given. It is very important to follow proper laser safety procedures during this alignment procedure. Please consult with your safety office or a laser safety reference<sup>22</sup> for complete instructions.

A few basic reminders are still in order here. The minimum laser power needed to image the beam should be used throughout the alignment procedure. Thorough checks should be made for stray beams and all stray beams should be blocked. Apertures should also be installed to prevent misaligned beams from causing dangerous strays. Except where absolutely required, the laser beam should be kept parallel to the ground and well below eye level. Eyes should be kept above the laser beam level whenever the laser beam is on. Laser safety goggles should be used at all times the laser is on. Be careful!

### A. Initial preparations

If the optics being used in the experiment are not new, an initial cleaning of the lenses and mirrors is strongly suggested. This includes the optical components in the microscope itself.

The trajectory of the light is controlled by reflecting the light from mirrors held in adjustable mounts. Each mount offers independent control of the angle between the mirror and two orthogonal axes. All of our mirrors are mounted in such mounts. Consequently, a pair of mirrors allows us to independently control the position and angle of the laser beam at any optical element.

The optical path from the laser to the microscope should be laid out with sufficient space between the laser and the telescope (see Fig. 5). It is also convenient to have a mirror between the curvature lens ( $L_3$ ) and the pinhole in order to align the focused spot onto the pinhole. Finally, it is convenient to have another mirror between the pinhole and the input of the microscope. We used a dichroic beamsplitter as

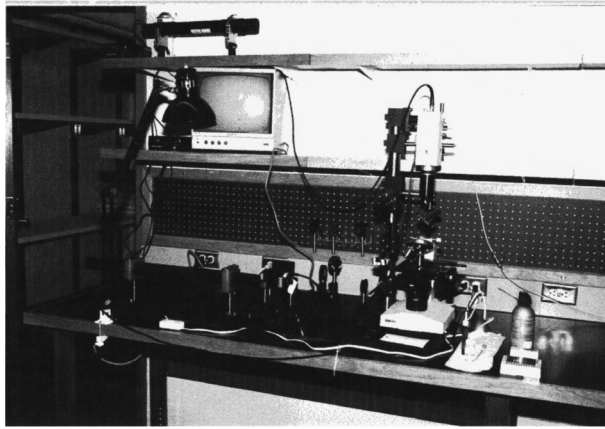


Fig. 6. Photograph of a simple optical tweezer setup. The He-Ne laser is seen on the left side of the photograph and the microscope on the right. The microscope's trinocular head has been removed and the CCD camera is supported by a 2-in. steel post located just to the left and behind the microscope. The same post is also used to support  $m_3$ ,  $m_4$ ,  $m_5$ ,  $L_3$ , and the pinhole. This built on a 24×36 in. optical breadboard to leave room for future enhancements, however, it could easily fit onto an 18×24 in. breadboard.

this final mirror. No lenses should be in the path at the start of the alignment procedure, including the microscope objective and eyepieces.

In our setups, the laser and the optics through  $L_2$  are supported in commercial optics mounts that are bolted to an optics breadboard. The mounts for  $L_3$ ,  $m_3$ ,  $m_4$  and the pinhole are mounted to a large post, and the video camera, video adapter, and  $m_5$  are mounted to a second large post. A photograph of one of these setups is shown in Fig. 6.

## B. Rough alignment

The mirrors should then be used to send the laser beam along the proposed optical path and to center it in the empty hole left by the objective. To allow for the widest adjustment range, the beam should also be centered on all of the mirrors. Make sure to allow sufficient space for the telescope and curvature adjusting lenses.

The position and angle of the laser beam entering the microscope can be adjusted with the aid of a microscope slide held flat against the microscope's translation stage: The trapping light should be adjusted so that it reflects off the microscope slide and returns back on its initial path. This is conveniently checked using an index card with a small hole in it: The forward propagating beam will pass through the hole and the backward propagating beam will appear on the card. After adjusting the reflection, the position of the beam should be checked to ensure that it is still centered on the screw mount that will hold the objective.

As shown in Fig. 5, it is convenient to have a pair of mirrors just before the objective ( $m_4$  and  $m_5$ ). One mirror ( $m_5$ ) is close to the objective and therefore has a large effect on the angle of the beam entering the objective, but only a small effect on the beam position. The second mirror ( $m_4$ ) is further away and so has a larger effect on the position of the beam at the objective, but only a small effect on the beam angle. Thus,  $m_5$  would be used to adjust the angle of the beam and  $m_4$  would be used to recenter the beam in the objective.

Next, the lenses need to be inserted one at a time into the beam path. When each lens is inserted, it first should be centered on the incoming light beam; then the lens is adjusted so that the light reflecting off the lens returns directly back on itself. This indicates that the face of the lens is perpendicular to the laser beam and well centered. If these steps are followed, the beam path with and without the lenses should be almost the same.

The lens closest to the laser,  $L_1$ , should be inserted first. The second lens in the telescope,  $L_2$ , should be inserted next, and the distance between the two lenses should be adjusted until the beam coming out of the telescope is collimated and the half-width of the beam at the output of the telescope is 0.75 cm.<sup>23</sup> The curvature adjusting lens,  $L_3$ , should then be inserted and aligned.

The location of the curvature matching lens can be checked by inserting a 40 $\mu$ m pinhole 16 cm from the rear of the objective. The final alignment of the laser beam through the pinhole should be done with the mirror just after the curvature lens,  $m_4$ . The position of the curvature lens,  $L_3$ , should then be carefully adjusted so that approximately 75% of the laser beam passes through the pinhole using only  $m_4$  to center the beam on the pinhole. Once the curvature matching lens has been appropriately positioned, the pinhole can be removed and the beam realigned through the microscope only using  $m_4$ .

The objective can then be inserted into the microscope. The laser light transmitted by the objective should be bright and symmetrical. It is easiest to view this beam when the microscope condenser is removed. If the beam from the objective is not symmetric, small adjustments can be made to the final positioning mirror,  $m_5$ , and the position of the microscope to achieve this. Finally, the condenser should be reinserted into the microscope.

## VI. TRAPPING PROCEDURE

### A. Test sample

Three-micron polystyrene spheres make excellent test objects for aligning the imaging system and for setting up the initial trap. A mixture of water and spheres should be prepared as suggested in Appendix B. Approximately 40  $\mu$ l of the mixture (one drop from a Pasteur pipette) should be placed on a microscope slide, which should then be covered with a cover slip. A small drop of low viscosity index matching fluid should be placed on the center of the top of the cover slip, the slide should be inserted into the sample holder on the microscope, and the imaging lighting should be turned on. To increase the lifetime of the slide, the edges of the slide can be sealed. Otherwise, sample solution will need to be periodically added to the slide to replace the liquid lost to evaporation.

It is important that the thickness of the sample on the microscope slide be  $\leq 50 \mu$ m because the strength of the trap decreases as the focused spot is moved deeper into the water. This decrease in trap strength is due to spherical aberrations caused by refraction at the glass-water interface between the cover slip and the sample.<sup>11</sup> Since the polystyrene balls are denser than water, they will sink to the bottom of the slide where the trap is weakest, making them difficult to trap initially. The depth of the sample can be found by measuring

how far the sample stage must translate to move the focus from the lower surface of the cover slip to the top surface of the microscope slide.

## B. Preparations

With the laser either blocked or off, move the sample holder so that the objective is in the middle of the slide. Adjust the focus until the spheres are clearly visible, then fine tune the focus so that spheres at the bottom of the sample are in sharp focus. If the microscope lighting is being used, the intensity of the light, the size of the aperture in the condenser, and condenser position should be adjusted so that the image contrast is maximized. Also, if a CCD camera is being used, the camera should be aligned at this time and adjusted so the focus of the video camera and the focus through the eyepiece are the same.

The next step is to find the trap position in the imaging field. Since this procedure requires the filtering to be adjusted so that the trapping beam is visible, it should only be done using a CCD camera. First, turn off the condenser illumination. Second, turn the laser on at a very low power level or if the power level of the laser cannot be adjusted, strongly attenuate the laser. Third, while slowly adjusting the focus up and down a small amount, look for a dim spot with the CCD camera (set for maximum sensitivity) which corresponds to the trapping light beam reflecting off the water-glass interface at the bottom of the sample. If none can be seen, the laser power can be increased until the focused spot is observed. Adjust the focus to maximize the intensity of this reflection, and mark the position of the trap on the CCD camera's monitor.

Turn the condenser back on. If the spheres on the bottom of the cell are not in focus, then the focal plane of the CCD camera and the trapping laser are not well aligned. This must be corrected or the trapped balls will be out of focus and not visible. The position of the pinhole and the alignment of the laser through the pinhole should be checked.

If the balls are in focus, then increase the laser power and move the sample holder down so that free floating spheres are now in focus. Gently move the sample holder around so that floating spheres are in focus and pass near the position of the trapping beam. Spheres should be pulled into the trapping beam and held there.

## C. Recognizing trapping

If the trapping is strong, the free floating balls should literally "jump" into the trap when they pass within a ball diameter or so of the trap position. Smooth lateral translations of the slide should not displace the sphere more than a ball diameter from the center of the trap. This is a test of trapping in the two transverse directions.

Weaker trapping can be observed by putting a free floating ball in sharp focus and slowly translating it through the trap. Even if the trap is very weak the ball can be seen momentarily "sticking" in the trap. It is important that the translations of the stage be very smooth, without abrupt starts or stops that could knock a ball out of the trap.

Figure 7 shows a demonstration of trapping using 3- $\mu\text{m}$  balls. In Fig. 7(a) the trapped ball is shown with a solid arrow, and a second ball that is stuck to the microscope slide is also visible (hollow arrow). In Fig. 7(b), the microscope stage has been moved down as indicated by the position of the stuck ball, but the position of the trapped ball is un-

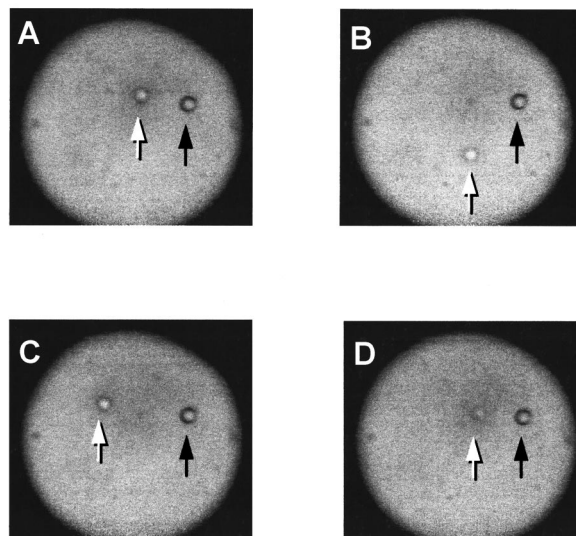


Fig. 7. Images from a CCD camera of the optical tweezer operation. A trapped 3- $\mu\text{m}$ -diam polystyrene ball (the solid arrow) and second ball stuck to the microscope slide (the hollow arrow) are shown at their starting position (A), as the microscope stage is moved horizontally [(B) and (C)] and as the stage is moved vertically (D). This demonstrates the three-dimensional trapping of the tweezers.

changed. Similarly, in Fig. 7(c) the microscope stage has been moved to the left and again the position of the trapped ball is unchanged, demonstrating two-dimensional trapping of the ball. Two-dimensional trapping can also be demonstrated by moving the trapping beam. Coarse movement of the trapping beam can be done by displacing  $L_2$  transverse to the optical beam or by changing the angle of  $m_3$ .

To demonstrate three-dimensional trapping, move the microscope focus up and down to show that the ball is trapped in the longitudinal direction as well as the two transverse directions. In this case it is very important that the translations be made smoothly and slowly since the trapping is weakest along the direction of propagation of the beam. While picking a ball up from the bottom of the sample, any sudden acceleration could easily dislodge the ball from the trap. Similarly, vibrations of the microscope can also dislodge the ball. If the ball is trapped in three dimensions, it will stay in focus as the microscope focus is moved vertically, while untrapped balls will slowly move out of focus, as shown in Fig. 7(d). It is not uncommon for a weak trap to be able to hold trap in two dimensions but not in three dimensions. It is also not uncommon for the trapped ball to be slightly out of focus even if it is stably trapped in all three dimensions, so careful observation of the ball can be required.

If the trapping is weak, spheres will linger near the trap or even remain in the trap, but they can be easily dislodged by translating the sample or by changing the focus. Cases of weak trapping can also be identified by the reorientation of clumps of balls as they move through the trap. In this case, check the laser power, make sure all the optics are clean, check the beam size at the back of the objective, and check the position of  $L_3$ .

If free floating spheres move into the trap, and then disappear, the trapping is probably stable only in the two transverse directions, but not the longitudinal direction. This can occur when the gradient forces are strong enough to hold the

ball laterally in the beam but not strong enough to overcome the scattering force in the direction of the laser beam. Dirty optics, an undersized trapping beam, or very large microscope slide-cover slip distances are frequently the problem.

Finally, if the trap appears to have no effect whatsoever, systematically recheck the alignment of all the components and recheck the laser power after the objective. Another possible cause of not trapping is a dry or very low water level in the microscope slide. Also, with time the balls tend to stick to the glass surfaces of the microscope slide. It is usually not possible to dislodge these balls with even the strongest optical tweezers.

Additional troubleshooting information is also available at our web site, <http://atom.harvard.edu/~tweezer>.

#### D. Trap calibration

One convenient method for calibrating the transverse strength of the trap is to measure the “escape” velocity of the ball as the microscope slide is translated horizontally. With the trapped ball well away from both the cover slip and microscope slide, the Stokes drag on the ball due to the water<sup>24</sup> can be calculated using

$$F_d = 6\pi\eta r v_c, \quad (2)$$

where  $F_d$  is the force due to drag,  $\eta$  is the viscosity of water which is approximately  $10^{-3}$  N s/m<sup>2</sup>,  $r$  is the radius of the sphere, and  $v_c$  is the velocity. For example, for a 3- $\mu$ m-diameter ball, the Stokes drag at 200  $\mu$ m/s is approximately 6 pN.

For this formula to be valid, the ball must be several ball diameters from the cover slip or slide to prevent surface effects from affecting the viscous drag. Further, since spherical aberrations will reduce the strength of the trap with increasing depth, the highest trap strengths occur a few ball diameters below the cover slip.

Measurement of the escape velocity from the trap can be conveniently done by videotaping the output of the CCD camera. With a ball trapped, the microscope stage is smoothly accelerated until the ball falls out of the trap. The translation velocity can be found by measuring the displacement of a fixed reference, typically a ball stuck to the microscope slide, between successive video frames just prior to the ball falling out of the trap. Calibration of the translation distance can be done by either measuring the size of a known object, for example, monodispersed polystyrene spheres, or by simultaneously measuring a displacement of the microscope stage and the displacement observed on the video monitor.

#### E. Optimizing the trap

In order to get the best trapping, some fine tuning of the trap is usually required. The two main adjustable parameters are the position of the curvature lens and the separation between the two lenses in the telescope. The position of the curvature lens adjusts the position of the trap relative to the eyepiece or camera focus. The distance between the lenses in the telescope controls the size of the beam at the back of the objective.

If trapped spheres are not in sharp focus, the position of the curvature lens,  $L_3$  in Fig. 5, should be adjusted so that the trap and the image focus are in the same horizontal plane. The procedure is to iteratively trap a ball, check the image,

and move the lens to improve the focus. If the curvature lens is moved very carefully, you might be able to keep a ball in the trap as the lens position is adjusted. Typically this lens is moved at most 1–2 cm.

Once the trap and image are in the same plane, the telescope separation should be adjusted to change the spot size at the back of the objective,  $d_{obj}$ , to maximize trap depth. If  $d_{obj}$  is not optimized, trapping occurs only if the trap is very close to the bottom of the cover slip, e.g., within 20  $\mu$ m. In contrast, a well optimized trap will confine particles even if the focused spot is more than 100  $\mu$ m below the bottom of the cover slip. The procedure for optimizing  $d_{obj}$  is to (a) trap ball, (b) measure maximum trapping distance below cover slip, (c) change  $d_{obj}$ , e.g., increase  $d_{obj}$ , (d) trap ball, (e) re-measure maximum trapping distance. If the distance increased, go to (c) and continue changing  $d_{obj}$  in the same way, e.g., continue to increase  $d_{obj}$ . If the distance decreased, go to (c) and reverse the direction of changing  $d_{obj}$ , e.g., start to decrease  $d_{obj}$ .

### VII. SUGGESTED EXPERIMENTS

There are a wide assortment of experiments that can be done with even a simple optical tweezer. While it is beyond the scope of this paper to summarize all the possibilities, this section is intended to stimulate ideas.

#### A. Trap strength measurements

Measuring the transverse trapping strength of optical tweezers as a function of various parameters provides a good opportunity to obtain experience with tweezer based measurements and offers useful information for planning future experiments. Measuring the trap depth in the transverse direction is discussed in Sec. VI D. The measurements in that section can be made as a function of the sample parameters such as: sphere size, sphere material, solution composition, and distance below the cover slip. These experiments are important in order to calibrate the forces used in the measurements suggested in the following sections.

#### B. Tweezer based measurements of motility

The motility of cells, for example sperm, can be measured by finding the minimum trap depth required to hold them, where the trap depth is controlled by varying the power of the trapping laser.<sup>2,25</sup> The motility of different organisms as a function of environmental conditions can be measured. This provides information on the effects of temperature, salinity, pH, etc., on motility that may for example provide useful information on the control of fertility.

#### C. Tweezer based measurements of the elasticity of cells

Cells can be distorted by optical tweezers in various ways. For example, the cell can be pressed against surfaces with various morphologies or the cell can be trapped at multiple points and the trapped points can be translated, resulting in cellular distortion.<sup>26</sup> The flexibility of certain cells, e.g., red blood cells, is important for their biological function.

#### D. Tweezer based control of cell morphology

The morphology of cells can be controlled by pressing trapped cells against surfaces with various morphologies, or by trapping a cell at multiple points and translating the rela-

tive position of the trapped points. Some distortions of cell shape have already been shown to have a significant impact on cell viability,<sup>27</sup> but more detailed studies of the impact of morphology on cell viability may yield important information.

### E. Tweezer based measurements of the elasticity of polymers

Though single strands of DNA are too small to manipulate directly with optical tweezers, they can be manipulated if they are attached to larger objects, such as polystyrene spheres, that can be trapped.<sup>8</sup> In such experiments, one end of the strand is attached to a microscope slide and the other is attached to a polystyrene ball. The elongation of the strand is then measured as a function of the applied force (controlled by the intensity of the laser used for the trap). One measurement that can be done in this way is the elasticity of the DNA strands under various environmental conditions.

### F. Tweezer based measurements of compliance

The compliance of the flagella on bacteria can also be measured using optical tweezers. The flagella are responsible for the swimming of the bacteria and the compliance of these organelles has been correlated with the health of the bacteria.<sup>4</sup> To measure the compliance of the flagella, a single flagellum from a bacterium is stuck to a surface, and then the bacterium is rotated about this flagellum. When the bacterium is released, the number of rotations that the bacterium springs back are measured. The compliance as a function of environmental variables such as temperature, salinity, and pH can be measured to determine the effects of environmental variables on the health of the cell.

## VIII. OTHER TWEezer CONFIGURATIONS AND ENHANCEMENTS

The use of the microscope is not really required for the tweezers, and it may be advantageous in some situations to eliminate the microscope altogether. The microscope objective can be mounted in a commercial optics mount, and a three-dimensional translation stage can be used to hold and coarsely manipulate the sample. Translation stages designed to align fiber optics work well as sample manipulators since they translate the sample smoothly and offer submicron positioning (e.g., Thorlabs MDT 612 Fiber Launch system). Many fiber mounts are also compatible with stepper motors and piezoelectric transducers that can provide accurate electronic position control.

If the microscope is eliminated, it is also easy to construct an “inverted” setup with the trapping light entering the sample cell from below, rather than above. Since most objects to be trapped are denser than water they will sink to the bottom, so, in this configuration, they will be against the cover slip where the trap is strongest. Hence, with this configuration very thick sample cells can easily be used.

The ability to hold multiple objects or a single object at multiple points increases the range of experiments that can be done. Collision experiments between trapped objects require a minimum of two beams<sup>28</sup> and orientation experiments can require three or more. The simplest method for generating a second trap is to add a second, independently steered trapping beam. If the two beams have opposite polarizations, a polarizing beam splitter can be used to combine

the beams with minimal power loss. It is convenient to combine the beams just before the lens  $L_3$ . Larger numbers of independently controlled traps can be generated by using acousto-optic modulators.<sup>29</sup> When these multiple traps are generated from a single laser using acousto-optic modulators, very precise two-dimensional control of the relative position and velocity of these traps can be obtained even in an apparatus with significant mechanical vibrations. Subnanometer differential position control should be possible. Using our apparatus we have demonstrated five simultaneous, independently steered traps. We have used these traps to control the collisions between several trapped particles. The two acousto-optic modulator systems required for this cost approximately \$10,000. One-dimensional control would require only a single acousto-optic modulator.

Other interesting enhancements that can be considered are improved beam steering<sup>30</sup> and direct measurement of the forces applied by the tweezers.<sup>31</sup>

## IX. SUMMARY

In this paper we have described how to construct a simple optical tweezer using a moderate power laser and a low-cost trinocular microscope. We have also suggested a variety of experiments that can be done using this apparatus.

## ACKNOWLEDGMENTS

This work was funded in part by NSF Grant No. PHY-9312572. The authors would like to thank Seok-Ki Choi, Mathai Mammen, George M. Whitesides, Kris Helmersen, Ben Davies, and Francisco Ponce for their assistance.

## APPENDIX A: OPTICS

In geometric optics, a lens in the  $z = z_{\text{lens}}$  plane that is centered on the  $z$  axis will focus a collimated beam, i.e., a beam composed of a collection of parallel rays, propagating in the  $+z$  direction to a point on the  $z$  axis. This focused spot will occur at  $z = z_{\text{lens}} + f$ , where  $f$  is the focal length of the lens. Similarly, a light beam that is propagating in the  $+z$  direction from a focus at  $z_f$  will be converted to a collimated beam by a lens with focal length  $f$  at  $z = z_f + f$ . More generally, an object a distance  $o$  from a lens of focal length  $f$  will be focused into an image a distance  $i$  from the lens, where

$$\frac{1}{i} + \frac{1}{o} = \frac{1}{f}$$

and the ratio of the size of the image to the size of the object is  $i/o$ . For the case of a collimated incident beam,  $o = \infty$ , so  $i = f$ . Similarly, for an incident beam with a focus at  $z_f = f$ ,

$$\frac{1}{i} + \frac{1}{o} = \frac{1}{i} + \frac{1}{f} \rightarrow i = \infty,$$

corresponding to a collimated beam.

The discussion above can be used to derive the magnification of a telescope composed of two convex lenses  $L_1$  and  $L_2$ . If a collimated beam with diameter  $d_{\text{in}}$  is incident on lens  $L_1$  with focal length  $f_1$ , it will be focused at a distance  $f_1$  from  $L_1$ . If a second lens,  $L_2$  with focal length  $f_2$  is placed a distance  $f_2$  from the focus ( $f_1 + f_2$  from  $L_1$ ), the

light from  $L_2$  will be collimated and have a diameter  $d_2 = d_1 f_2 / f_1 = M d_1$ , where  $M$  is the magnification of the telescope.

Geometric optics ignores the wave nature of light. Geometric optics can be considered the limit of wave optics when the wavelength of the light approaches zero. The diffraction associated with the finite wavelength of light implies that contrary to geometric optics, no light beam can be focused to a spot with zero size. A collimated light beam with a diameter  $d$  that is incident on an ideal lens with focal length  $f$  can only be focused to a spot size with radius  $w_0 = f\lambda/d$ , where  $\lambda$  is the wavelength of the light. The size of a laser beam is slightly ambiguous since a typical laser beam propagating in the  $z$  direction has a Gaussian intensity profile  $I(x,y) = I_0 \exp[-2(x^2+y^2)/w_0^2]$ . The parameter  $w_0$  is called the waist and is usually referred to as the size of the laser beam.

In wave optics, a light beam is characterized not only by its size but also by the spatial dependence of the phase of the beam. For a beam propagating away from a tightly focused spot, the contours of constant phase are approximately spherical with a radius of curvature equal to the distance from the focused spot. The point at which a lens will focus an incident light beam depends on the radius of curvature of the incoming light: The focusing of a laser beam with a radius of curvature  $R$  at a lens with focal length  $f$  will be approximately the same as the focusing predicted by geometric optics for an image at a position  $i=R$ . A more correct and detailed description of the propagation of laser beams can be obtained using the *ABCD* matrices.<sup>17</sup>

## APPENDIX B: BALL CHOICE AND SOLUTION

Polystyrene balls make a good choice for initial trapping experiments. They are available in a variety of sizes, have a long storage life, and can be trapped with a variety of wavelengths without damage. There are a large number of suppliers of these balls including: Bangs Laboratories, Inc., Fishers, IN, Polyscience, Inc., Warrington, PA.

If these balls are simply added to a distilled water solution, they tend to clump together and stick to the cover slip and slide. To minimize this behavior we suspend the balls in a phosphate-buffered saline solution (PBS). Similar solutions are commonly used for suspending biological specimens. The formula for PBS is given below:

- 0.8% NaCl,
- 0.02% KCL,
- 0.02 M PO<sub>4</sub>, pH 7.3 (percentage by weight).

In addition to using PBS, an additional antistick additive is usually used. For nonbiological specimens this is usually  $\approx 1\%$  polyethylene glycol. For biological specimens, polyethylene glycol cannot be used and bovine serum albumin (BSA) can be used instead. As with all chemicals, the material safety data sheets should always be carefully reviewed before using them.

<sup>1</sup>A. Ashkin, J. M. Dziedzic, J. E. Bjorkholm, and Steven Chu, "Observation of a single-beam gradient force optical trap for dielectric particles," *Opt. Lett.* **11** (5), 288–291 (1986).

<sup>2</sup>A. Ashkin, J. M. Dziedzic, and T. Yamane, "Optical trapping and manipulation of single cells using infrared laser beams," *Nature (London)* **330**, 769–771 (1987).

<sup>3</sup>A. Ashkin and J. M. Dziedzic, "Optical trapping and manipulation of viruses and bacteria," *Science* **235**, 1517–1520 (1987).

<sup>4</sup>S. M. Block, D. F. Blair, and H. C. Berg, "Compliance of bacterial flagella

measured using optical tweezers," *Nature (London)* **338**, 514–518 (1989).

<sup>5</sup>M. W. Berns, W. H. Wright, B. J. Tramberger, G. A. Profeta, J. J. Andrews, and R. J. Walters, "Use of a laser-induced force trap to study chromosome movement on the mitotic spindle," *Proc. Natl. Acad. Sci. USA* **86**, 4539–4543 (1989).

<sup>6</sup>A. Ashkin and J. M. Dziedzic, "Internal cell manipulation using infrared laser traps," *Proc. Natl. Acad. Sci. USA* **86**, 7914–7918 (1989).

<sup>7</sup>Karel Svoboda and Steven M. Block, "Optical Trapping of Metallic Rayleigh Particles," *Opt. Lett.* **19** (13), 930–932 (1994).

<sup>8</sup>Steven Chu, "Laser manipulation of atoms and particles," *Science* **252**, 861–866 (1991).

<sup>9</sup>Karel Svoboda and Steven M. Block, "Biological Applications of Optical Forces," *Annu. Rev. Biophys. Biomol. Struct.* **23**, 247–285 (1994).

<sup>10</sup>J. C. Crocker and D. G. Grier, "Microscopic measurement of the pair interaction potential of charge-stabilized colloid," *Phys. Rev. Lett.* **73**, 352–355 (1994).

<sup>11</sup>W. H. Wright, G. J. Sonek, and M. W. Berns, "Parametric study of the force on a microsphere held by optical tweezers," *Appl. Opt.* **33** (9), 1735–1748 (1994).

<sup>12</sup>If the index of refraction of the object is smaller than the index of the surrounding medium, then the refraction would result in a force that ejects the particle from the trap.

<sup>13</sup>A. Ashkin, "Forces of a single-beam gradient laser trap on a dielectric sphere in the ray optics regime," *Biophys. J.* **61**, 569–582 (1992).

<sup>14</sup>A more detailed version of this derivation can be found on our web site at <http://atomsun.harvard.edu/~tweezer>.

<sup>15</sup>Edward M. Purcell, *Electricity and Magnetism* (McGraw–Hill, New York, 1985), pp. 348–370.

<sup>16</sup>John David Jackson, *Classical Electrodynamics* (Wiley, New York, 1975), pp. 269–298.

<sup>17</sup>For more information of Gaussian optics please see Chap. 2 in A. Yariv, *Optical Electronics* (Wiley, New York, 1985), 3rd ed.

<sup>18</sup>Frederick Reif, *Statistical Physics* (McGraw–Hill, New York, 1967).

<sup>19</sup>A. Ashkin, "Forces of a single-beam gradient laser trap on a dielectric sphere in the ray optics regime," *Biophys. J.* **61**, 569–582 (1992).

<sup>20</sup>In this discussion we characterize the laser beam with a definite diameter. Typical laser beams propagating in the  $z$  direction have an intensity profile  $I(x,y) = I_0 \exp[-2(x^2+y^2)/w_0^2]$ . Best trapping is obtained when the waist  $w_0$  is approximately  $d_{obj}/2$ .

<sup>21</sup>An anamorphic prism uses a pair of glass prisms to compress or expand an optical beam along one axis. For example, see Melles–Griot part number 06 GPA 004.

<sup>22</sup>American National Standards Institute, American National Standard for the Safe Use of Lasers: ANSI Z 136.1 (1993), Laser Institute of America, New York, NY (1993). There are also a number of websites with information, for example, <http://www.osha-slc.gov/> by OSHA and <http://www.creol.ucf.edu/lia/> from the Laser Institute of America.

<sup>23</sup>If the output of the laser was not collimated, the magnification of the telescope may not be  $L_2/L_1$ . The values of lenses  $L_1$  and  $L_2$  should be changed until the collimated output of the telescope has a half-width of 0.75 cm.

<sup>24</sup>G. K. Batchelor, *An Introduction to Fluid Dynamics* (Cambridge U.P., Cambridge, 1991).

<sup>25</sup>Y. Tadir, W. H. Wright, O. Vafa, T. Ord, R. H. Asch, and M. W. Berns, "Force generation by human sperm correlated to velocity and determined using a laser generated optical trap," *Fertil. Steril.* **53**, 944–947 (1989).

<sup>26</sup>P. J. H. Bronkhorst, G. J. Streekstra, J. Grimbergen, E. J. Nijhof, J. J. Sixma, and G. J. Brakenhoff, "A New Method to Study Shape Recovery of Red Blood Cells Using Multiple Optical Trapping," *Biophys. J.* **69**, 1666–1673 (1995).

<sup>27</sup>Christofer S. Chen, Milan Mrksich, Sui Huang, George M. Whitesides, and Donald E. Ingber, "Geometric control of cell life and death," *Science* **276**, 5317 (1997).

<sup>28</sup>Mathai Mammen, Kristian Helmersson, Rani Kishore, Seok-Ki Choi, William D. Phillips, and George M. Whitesides, "Optically controlled collisions of biological objects to evaluate potent polyvalent inhibitors of virus-cell adhesion," *Chem. Biol.* **3**, 757–763 (1996).

<sup>29</sup>Koen Visscher, Steven P. Gross, and Steven M. Block, "Construction of Multiple-Beam Optical Traps with Nanometer-Resolution Position Sensing," *J. Select. Topics Quantum Electron.* **2** (4), 1066–1075 (1996).

<sup>30</sup>Erik Fällman and Ove Axner, "Design for Fully Steerable Dual Trap Optical Tweezers," *Appl. Opt.* **36** (10), 2107–2113 (1997).

<sup>31</sup>K. Svoboda, C. F. Schmidt, B. J. Schnapp, and S. M. Block, "Direct observation of kinesin stepping by optical trapping interferometry," *Nature (London)* **365**, 721–27 (1993).